

Quantifying seasonal precipitation using high-resolution carbon isotope analyses in evergreen wood

Brian A. Schubert^{*}, A. Hope Jahren

Department of Geology and Geophysics, University of Hawaii, Honolulu, HI 96822, USA

Received 8 March 2011; accepted in revised form 1 August 2011; available online 6 August 2011

Abstract

High-resolution natural abundance stable carbon isotope analyses across annual growth rings in evergreen trees reveal a cyclic increase and decrease in the measured carbon isotopic composition ($\delta^{13}\text{C}$), but the causes of this pattern are poorly understood. We compiled new and published high-resolution $\delta^{13}\text{C}$ data from across annual growth rings of 33 modern evergreen trees from 10 genera and 15 globally distributed sites to quantify the parameters that affect the observed $\delta^{13}\text{C}$ pattern. Across a broad range of latitude, temperature, and precipitation regimes, we found that the average, measured seasonal change in $\delta^{13}\text{C}$ ($\Delta\delta^{13}\text{C}_{\text{meas}}$, ‰) within tree rings of evergreen species reflects changes in the carbon isotopic composition of atmospheric carbon dioxide ($\Delta\delta^{13}\text{C}_{\text{CO}_2}$) and changes in seasonal precipitation (ΔP) according to the following equation: $\Delta\delta^{13}\text{C}_{\text{meas}} = \Delta\delta^{13}\text{C}_{\text{CO}_2} - 0.82(\Delta P) + 0.73$; $R^2 = 0.96$. Seasonal changes in temperature, pCO_2 , and light levels were not found to significantly affect $\Delta\delta^{13}\text{C}_{\text{meas}}$. We propose that this relationship can be used to quantify seasonal patterns in paleoprecipitation from intra-ring profiles of $\delta^{13}\text{C}$ measured from non-permineralized, fossil wood.

© 2011 Elsevier Ltd. All rights reserved.

1. INTRODUCTION

The main vertical trunk of a tree contains tissue that transports nutrients up to leaves and down to roots. This tissue is continuously augmented by new tissue, which then takes over the transport function leaving the older tissue to support the structure of the increasing canopy. This process produces wood with ringed anatomy such that the oldest tissue of the tree comprises its center, while the youngest tissue increases its diameter. In both gymnosperm and angiosperm trees, an abrupt or gradual change in the density, shape, and size of cells often follows an annual pattern. A cross section of ringed wood represents a continuous record of tissue synthesized across a time span of up to thousands of years (Currey, 1965). The width of these rings and the density of the wood are commonly used to interpret past climates (e.g., Hughes et al., 1984;

Till and Guiot, 1990; Lara and Villalba, 1993; Grudd et al., 2002) including climatic aberrations that may have contributed to the decline of ancient cultures (Buckley et al., 2010; Stahle et al., 2011). Decades of research have also investigated the potential for ring-width and anatomical aberrations to record resource availability (Piutti and Cescatti, 1997; Tognetti et al., 2000; Cherubini et al., 2003; Galle et al., 2010) and pathogen occurrence (Oberhuber et al., 1999; Cherubini et al., 2002) through time. Similarly, radiocarbon (Suess, 1980; Solanki et al., 2004) and heavy metal (Tommasini et al., 2000; Prapaipong et al., 2008) concentrations have been used to interpret sun spot activity and global elemental cycling across tens to thousands of years of Earth history.

Environmental parameters also affect the partitioning of carbon stable isotopes into plant tissues (Farquhar et al., 1989; Dawson et al., 2002). Workers have used ring-to-ring records of natural abundance stable carbon isotope ratios ($\delta^{13}\text{C}$) to interpret annual climate trends and variability across multiple consecutive years (reviewed by McCarroll and Loader, 2004). Such studies have related $\delta^{13}\text{C}$ values to paleotemperature (Jędrysek et al., 2003; Gagen et al.,

^{*} Corresponding author. Tel.: +1 808 956 0457; fax: +1 808 956 5512.

E-mail address: bschube@hawaii.edu (B.A. Schubert).

2007), paleoprecipitation (Norström et al., 2005; Gebrekirstos et al., 2009), paleosunshine (McCarroll and Pawellek, 2001; McCarroll et al., 2003; Young et al., 2010), and paleohumidity (Edwards et al., 2000). Still, a unifying interpretive model linking stable carbon isotopes in tree rings to environmental conditions is lacking (McCarroll and Loader, 2004). Comparison of the ring-to-ring $\delta^{13}\text{C}$ values to the known climatic history in living trees has revealed that no single climatic control is sufficient to account for the entire $\delta^{13}\text{C}$ signal (Gagen et al., 2007).

2. CARBON ISOTOPES IN WOOD

Fundamental understanding of carbon isotope fractionation in plants is based on the model proposed by Farquhar et al. (1982):

$$\delta^{13}\text{C} = \delta^{13}\text{C}_{\text{CO}_2} - a - (b - a)(c_i/c_a) \quad (1)$$

where $\delta^{13}\text{C}_{\text{CO}_2}$ and $\delta^{13}\text{C}$ represent the carbon stable isotope composition of atmospheric CO_2 and of the resulting plant tissue, respectively; a and b are constants that encompass the isotopic fractionation inherent to gaseous diffusion and enzymatic carboxylation, respectively; (c_i/c_a) is a unitless scalar that represents the partial pressure of CO_2 within the stomatal chamber (c_i) relative to the partial pressure of CO_2 in the external atmosphere (c_a) as regulated by stomatal conductance (Appendix A). Regulation of stomatal openings is the primary mechanism that all vascular plants employ to adjust in response to changing environmental conditions (Brodribb and McAdam, 2011). Multiple studies have shown that water, temperature, light, and the atmospheric concentration of CO_2 alter the carbon isotopic composition of plant tissues and thus c_i/c_a (Ehleringer et al., 1986; Ehleringer and Cooper, 1988; Farquhar et al., 1989; Toft et al., 1989; Zimmerman and Ehleringer, 1990; Körner et al., 1991; Van de Water et al., 1994; Feng and Epstein, 1995; Kelly and Woodward, 1995; Arens et al., 2000; Bowling et al., 2002; Yin et al., 2005, 2009; Aranda et al., 2007; Cernusak et al., 2009; Treydte et al., 2009; Kranabetter et al., 2010) (Table 1).

For tree-ring tissue, workers have proposed that the dominant influence on the $\delta^{13}\text{C}$ value is photosynthetic rate (sunshine and temperature) or stomatal conductance (antecedent rainfall and air relative humidity), depending on the site (McCarroll and Pawellek, 2001; Young et al., 2010). Direct correlation between the $\delta^{13}\text{C}$ value in tissues and climate parameters (e.g., temperature, mean annual

precipitation, etc.) is complicated by differences in the $\delta^{13}\text{C}$ value measured among species growing at the same site, likely caused by differences in water transport systems and leaf morphologies (e.g., needle vs. broadleaf) (McCarroll and Loader, 2004). The $\delta^{13}\text{C}$ value of wood can also vary among species growing within a single site across the same time period (Leavitt, 2002, 2010) due to differences in c_i/c_a (Gebrekirstos et al., 2011). These results, taken together, have led to the belief that wood $\delta^{13}\text{C}$ values, in isolation, are unlikely to be able to be used as a quantitative metric to solve for environmental variables (McCarroll and Loader, 2004).

In the last 20 years, researchers have improved upon single ring-measurements of $\delta^{13}\text{C}$ in plant tissue by developing a variety of methods for subsampling across single tree rings, including hand-slicing (Leavitt and Long, 1991; Leavitt, 2002, 2007; Kagawa, 2003; Jahren and Sternberg, 2008; Roden et al., 2009), microtome sectioning (Barbour et al., 2002; Helle and Schleser, 2004; Nakatsuka et al., 2004), and laser ablation (Schulze et al., 2004; Vaganov et al., 2009; Battipaglia et al., 2010). Modern tree-rings from deciduous and evergreen species have been analyzed for $\delta^{13}\text{C}$ at ~ 10 – $240 \mu\text{m}$ increments, which translates into as many as ~ 300 analyses per tree ring (e.g., Barbour et al., 2002; Helle and Schleser, 2004). Such high-resolution sampling reveals a clear, annual pattern in both modern (e.g., Helle and Schleser, 2004) and fossil (Jahren and Sternberg, 2008) deciduous wood that reflects the switchover from storage compounds to active photosynthate during the growing season. Because stored carbon compounds are isotopically heavy compared to recent photosynthate, $\delta^{13}\text{C}$ values in deciduous wood decrease across a single ring, in the direction of growth (Fig. 1a). Evergreen wood shows a markedly different pattern, with $\delta^{13}\text{C}$ values increasing and decreasing across a single ring (Fig. 1b). Previous work on a limited number of rings has shown that the change in $\delta^{13}\text{C}$ across a growth ring in evergreen wood may reflect climate (Leavitt and Long, 1991; Walcroft et al., 1997; Barbour et al., 2002; Leavitt, 2002), however no quantitative relationships have been made between climate parameters and this seasonal change. Site-specific interpretations describing local climatic control over evergreen isotopic patterns have been proposed (Leavitt, 2002; Verheyden et al., 2004; Roden et al., 2009), but no relationship between climate and within-ring $\delta^{13}\text{C}$ patterns in evergreen wood has been developed that can be applied globally. Maximum $\delta^{13}\text{C}$ values in evergreen trees have been shown to correlate with a wide variety of parameters including the highest vapor-pressure deficit, highest temperatures, lowest soil moisture, or highest $\delta^{13}\text{CO}_2$ values of the annual cycle (Wilson and Grinstead, 1977; Leavitt and Long, 1991; Kitagawa and Wada, 1993; Sheu et al., 1996; Barbour et al., 2002; Leavitt, 2002, 2007; Eilmann et al., 2010; Klein et al., 2005) (Table 1).

To quantify the variables that control the seasonal $\delta^{13}\text{C}$ pattern in evergreen trees and to test the potential for relative changes in $\delta^{13}\text{C}$ measured across annual growth rings to be used as a paleoclimate proxy, we compiled high-resolution, intra-ring $\delta^{13}\text{C}$ data from published and new analyses of angiosperm and gymnosperm evergreen species

Table 1

General effect of environmental parameters on the isotopic composition of plant tissue synthesized.

Environmental parameter	$\delta^{13}\text{C}$ synthesized
Increase in $\delta^{13}\text{C}_{\text{CO}_2}$ value	+
Increase in c_a	–
Increase in precipitation	–
Increase in available light	+
Increase in temperature	+/– ^a

+, increase; –, decrease

^a Schleser et al. (1999).

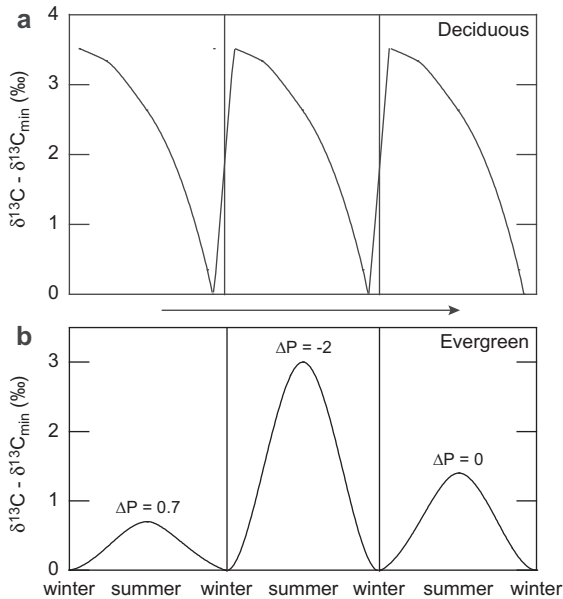


Fig. 1. Idealized $\delta^{13}\text{C}$ pattern across tree rings in (a) deciduous and (b) evergreen species growing at $\sim 50^\circ\text{N}$ latitude. Vertical lines mark annual boundaries. (a) Through the year, three phases are apparent in the intra-ring $\delta^{13}\text{C}$ pattern of deciduous tree rings as described by Helle and Schleser (2004): $\delta^{13}\text{C}$ enrichment during the early vegetation period, $\delta^{13}\text{C}$ decline during the main vegetation period, and $\delta^{13}\text{C}$ increase at the very end of the vegetation period. (b) The intra-ring $\delta^{13}\text{C}$ pattern of evergreen trees reflects environmental conditions. From left to right: ~ 2 times more precipitation in summer than winter ($\Delta P = 0.7$), ~ 7 times more precipitation in winter than summer ($\Delta P = -2$), and equal amounts of precipitation in summer and winter ($\Delta P = 0$). Note how the amplitude of the $\delta^{13}\text{C}$ pattern in evergreen trees for a given site changes due to changes in ΔP . Arrow indicates direction of growth.

growing in diverse terrestrial biomes around the world. We used this dataset to produce a multivariate, predictive relationship for paleoclimate by calculating how the relative seasonal change in $\delta^{13}\text{C}$ measured across tree rings is affected by relative changes in seasonal climate (precipitation and temperature), light, c_w , $\delta^{13}\text{C}_{\text{CO}_2}$, and post-photosynthetic physiological processes.

3. METHODS

We compiled high-resolution, intra-ring, $\delta^{13}\text{C}$ data published since 2000 for 33 evergreen trees from 15 globally-distributed sites (Fig. 2, and Tables 2 and EA1). All isotope data represent $\delta^{13}\text{C}$ determinations in bulk wood, except for the studies reporting *Shorea* (holocellulose, Ohashi et al., 2009), *Podocarpus* (α -cellulose, Poussart et al., 2004) and *Arbutus* (bulk and cellulose, Battipaglia et al., 2010) trees. Multiple studies have demonstrated that there is a consistent isotopic offset between whole wood and cellulose fractions and therefore a similar intra-ring $\delta^{13}\text{C}$ pattern (Leavitt and Long, 1991; Verheyden et al., 2005; Pons and Helle, 2011). Because we wished to evaluate the change in $\delta^{13}\text{C}$ within entire rings, we excluded studies that only sampled earlywood and latewood, or were limited to

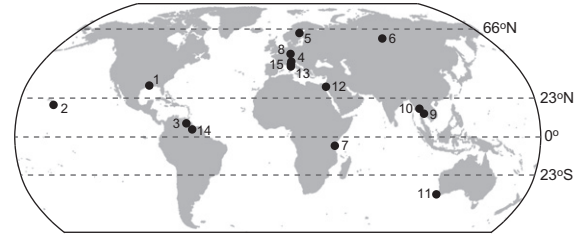


Fig. 2. Global distribution of the 15 sites from which high-resolution $\delta^{13}\text{C}$ tree-ring data were compiled for analysis. Sites are labeled according to the site numbers listed in Table 2.

measurements across only one or two rings per tree (Barbour et al., 2002; Leavitt, 2002, 2007; Eilmann et al., 2010). We excluded one study on *Sequoia* because the $\delta^{13}\text{C}$ value was greatly affected by significant seasonal fog within a unique hydrologic environment (Roden et al., 2009).

We augmented the dataset compiled from published literature with new measurements on *Pinus* and *Sophora* wood from Mississippi and Hawaii, USA, respectively, in order to increase coverage for temperate climate sites. For the wood samples from Mississippi and Hawaii, growth rings were subsampled by hand using a razor blade and weighed into pure tin capsules. We chose to measure $\delta^{13}\text{C}$ in whole-wood, not cellulose, to expedite high-resolution sampling (Schulze et al., 2004) and reduce bias (Walia et al., 2010). Bulk $\delta^{13}\text{C}$ values were determined using a Eurovector automated elemental analyzer (Eurovector Inc., Milan, Italy) coupled to an Isoprime isotope ratio mass spectrometer (Isoprime Ltd., Cheadle Hulme, UK) (Kraft et al., 2008). Each slice of Mississippi wood was homogenized and reported as the average of three replicate analyses; each slice of the Hawaii sample was analyzed in full. The analytical uncertainty associated with each measurement was $< 0.1\text{‰}$.

We measured the average, seasonal change in the $\delta^{13}\text{C}$ value ($\Delta\delta^{13}\text{C}_{\text{meas}}$) for each site by averaging the differences between the maximum $\delta^{13}\text{C}$ value of a given year ($\delta^{13}\text{C}_{\text{max}}$) and the preceding minimum $\delta^{13}\text{C}$ value of the annual cycle ($\delta^{13}\text{C}_{\text{min}}$) (Fig. 3). By studying relative changes in $\delta^{13}\text{C}$, rather than absolute $\delta^{13}\text{C}$ values, one can compare diverse species that may have different $\delta^{13}\text{C}$ values even when growing under the same conditions (Leavitt, 2002, 2010; McCarroll and Loader, 2004; Gebrekirstos et al., 2011). Verheyden et al. (2004) noted that although $\delta^{13}\text{C}$ values varied around the circumference of a tree, the seasonal changes in $\delta^{13}\text{C}$ were correspondent regardless of circumferential position.

$\delta^{13}\text{C}_{\text{max}}$, $\delta^{13}\text{C}_{\text{min}}$, and $\Delta\delta^{13}\text{C}_{\text{meas}}$ data for all tree rings are provided in Table EA1. In wood from 12 of the 15 sites, ring boundaries were determined visually by standard color and anatomical changes from earlywood to latewood. Within tropical lowland rainforest trees, however, annual ring patterns are commonly indistinct (Stahle, 1999). Therefore, for trees from Guyana [*Carapa* and *Goupia* (Pons and Helle, 2011)] and Thailand [*Shorea* (Ohashi et al., 2009) and *Podocarpus* (Poussart et al., 2004)], ring boundaries were defined by the isotopic pattern, as demonstrated within Leavitt and Long (1991).

Table 2
Tree-ring sampling data.

Site No.	Location	Genus	Conifer/angiosperm	No. trees	No. rings	No. $\delta^{13}\text{C}$ analyses	$\delta^{13}\text{C}$ analyses/ring	References ^c
1	Natchez State Park, Mississippi, USA; 31° 36' N, 91° 13' W	<i>Pinus</i>	Conifer	1	6	40	6.7	This study
2	Mauna Kea, Hawaii, USA; 19° 50' N, 155° 36' W	<i>Sophora</i>	Angiosperm	1	8	223	27.9	This study
3	Sierra de Lema, Venezuela; 6° 6' N, 61° 23' W	<i>Terminalia</i>	Angiosperm	1	21	68	3.2	Fichtler et al. (2010, Fig. 3b)
4	Renon, northern Italy; 46° 36' N, 11°28' E	<i>Picea</i>	Conifer	3	21	269	12.8	Vaganov et al. (2009, Fig. 7)
5	Flakaliden, northern Sweden; 64° 7' N, 19° 27' E	<i>Picea</i>	Conifer	3	16	168	10.5	Vaganov et al. (2009, Fig. 7)
6	Central Siberia; 60° 43' N, 89° 8' E	<i>Pinus</i>	Conifer	2	59	– ^b	– ^b	Schulze et al. (2004, Fig. 5 bulk, Fig. 6, Fig. 9 tree 16)
7	Gazi Bay, Kenya; 4° 25' S, 39° 30' E	<i>Rhizophora</i>	Angiosperm	3	26	464	17.8	Verheyden et al. (2004, Figs. 3 and 6)
8	Hainich, central Germany; 51° 4' N, 10° 27' E	<i>Picea</i>	Conifer	3	12	211	17.6	Vaganov et al. (2009, Fig. 7)
9	Nakhorn Ratchasima, NE Thailand; 14° 30' N, 101° 56' E	<i>Shorea</i>	Angiosperm	1	12	100 ^c	8.3	Ohashi et al. (2009, Fig. 4 SH8)
10	Chiang Mai, northern Thailand; 18° 30' N, 98° 30' E	<i>Podocarpus</i>	Conifer	1	6	52 ^d	8.7	Poussart et al. (2004, Fig. 6a)
11	Southwestern Australia; 33° 58' S, 115° 26' E	<i>Pinus</i>	Conifer	4 ^a	16	64	4.0	Warren et al. (2001, Fig. 5)
12	Yatir forest, Negev Desert, Israel; 31° 20' N, 35° 00' E	<i>Pinus</i>	Conifer	1	4	35	8.8	Klein et al. (2005, Fig. 3a control)
13	Elba, Italy; 42° 46' N, 10° 11' E	<i>Arbutus</i>	Angiosperm	4	14	119	8.5	Battipaglia et al. (2010, Figs. 6 and 7)
14	West Pibiri, central Guyana; 5° 2' N, 58° 37' W	<i>Carapa</i> <i>Goupia</i>	Angiosperm/ angiosperm	2/2 28/ 33	28/ 33	574/508	20.5/15.4	Pons and Helle (2011, Fig. 4)/ Pons and Helle (2011, Fig. 5)
15	Pisa, Italy; 43° 13' N, 10° 17' E	<i>Pinus</i>	Conifer	1 ^a	4	14	3.5	De Micco et al. (2007, Fig. 6)

^a Each was reported as a mean of 5 trees.

^b Not given in reference.

^c Holocellulose.

^d α -cellulose.

^e Figure information refers to the listed reference, not this study.

4. RESULTS AND ANALYSIS

The final dataset consisted of intra-ring $\delta^{13}\text{C}$ data across 286 complete tree rings from 33 evergreen trees growing at 15 globally distributed sites covering 98 degrees of latitude (Table 2). The climate in which the analyzed trees grew included arid, tropical, cold, and temperate environments (Peel et al., 2007; Table 3). The taxonomic diversity of the dataset was high; seven angiosperm genera (*Sophora*, *Terminalia*, *Rhizophora*, *Shorea*, *Arbutus*, *Carapa*, *Goupia*) and three conifer genera (*Picea*, *Pinus*, *Podocarpus*) were included (Table 2). Data for two genera (*Carapa* and *Goupia*) were combined for the Guyana site.

The isotope patterns in trees from all 15 sites showed an annually repeating increase and decrease in the $\delta^{13}\text{C}$ value (Fig. 4), similar to those noted within multiple previous studies (Wilson and Grinsted, 1977; Leavitt and Long, 1991; Kitagawa and Wada, 1993; Sheu et al., 1996; Barbour et al., 2002; Leavitt, 2002, 2007; Eilmann et al., 2010). Values of $\Delta\delta^{13}\text{C}_{\text{meas}}$ varied between 0.5 and 3.0‰ across all sites, with $\Delta\delta^{13}\text{C}_{\text{meas}}$ generally increasing as the average

$\delta^{13}\text{C}$ value for each site increased, however this relationship was not significant ($R^2 = 0.40$; $P = 0.14$, two-tailed). Although tree rings were not all sampled at the same resolution, there was no correlation between the number of subsamples per ring and $\Delta\delta^{13}\text{C}_{\text{meas}}$ ($R^2 = 0.09$). There is an inherent averaging of the $\delta^{13}\text{C}$ signal that takes place, however, when $\delta^{13}\text{C}$ measurements are not taken at the smallest increment possible. Thus, there is a potential to underestimate the maximum change in $\delta^{13}\text{C}$ ($\Delta\delta^{13}\text{C}_{\text{max}}$); only analysis at infinite resolution will result in $\Delta\delta^{13}\text{C}_{\text{max}} = \Delta\delta^{13}\text{C}_{\text{meas}}$. To illustrate this, we used our high-resolution $\delta^{13}\text{C}$ data across eight rings of a single *Sophora* tree growing in Hawaii (Fig. 4, Hawaii). This sample was sub-sectioned at an average of 27.9 measurements/ring (Table 2), which resulted in $\Delta\delta^{13}\text{C}_{\text{meas}} = 1.30\text{‰}$. We then took 3-, 5- and 7-point running averages across our data, which resulted in 9.3, 5.6, and 4.0 measurements per ring, respectively (Fig. 5). New estimates for $\Delta\delta^{13}\text{C}_{\text{meas}}$ were determined for each of these lower resolution data sets, a hyperbolic curve was fit through the data, and $\Delta\delta^{13}\text{C}_{\text{max}}$ was determined ($\Delta\delta^{13}\text{C}_{\text{max}} = 1.44\text{‰}$; the asymptote of the hyperbolic curve)

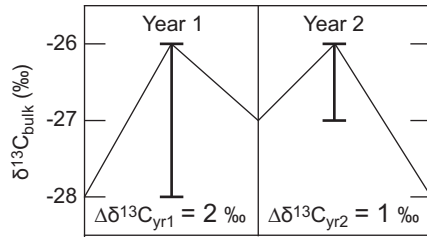


Fig. 3. Hypothetical isotope pattern across successive rings illustrates how the measured average seasonal change in $\delta^{13}\text{C}$ ($\Delta\delta^{13}\text{C}_{\text{meas}}$) was calculated for each site. The $\Delta\delta^{13}\text{C}$ value for each ring was calculated as the difference between the maximum $\delta^{13}\text{C}$ value of a given year and the preceding minimum $\delta^{13}\text{C}$ value of the annual cycle. These differences were then averaged for each site to obtain $\Delta\delta^{13}\text{C}_{\text{meas}}$; $\Delta\delta^{13}\text{C}_{\text{meas}}$ for this illustration is 1.5‰. Note that although the rings are mirror images of each other, they yield different $\Delta\delta^{13}\text{C}$ values for each year.

(Fig. 5). For this sample, we calculated that by sub-sectioning our core into 27.9 measurements/ring, $\sim 90\%$ of the $\delta^{13}\text{C}$ signal was recovered; by comparison, only half of the $\delta^{13}\text{C}$ signal would be achieved by dividing the rings into four sub-sections (Fig. 5). The full dataset analyzed here (Table 2), however, contains studies that targeted anatomical features within the wood, including changes in wood properties and intra-annual density fluctuations (IADFs) (Warren et al., 2001; De Micco et al., 2007; Battipaglia

et al., 2010). Features such as IADFs have been shown to contain $\delta^{13}\text{C}_{\text{max}}$ and $\delta^{13}\text{C}_{\text{min}}$ (Battipaglia et al., 2010); therefore, three $\delta^{13}\text{C}$ measurements taken in targeted sections of the wood (i.e., earlywood, IADF, latewood) will likely produce a higher value for $\Delta\delta^{13}\text{C}_{\text{meas}}$ than three evenly spaced measurements. Because the correction shown in Fig. 5 is specific to a single analysis, it cannot be applied consistently for all sites in our dataset. Therefore, our analysis of the $\Delta\delta^{13}\text{C}_{\text{meas}}$ data presented here does not apply a correction for the sample resolution. However, it may be warranted when analyzing a new substrate, to perform measurements at as high of resolution as possible in order to generate data as shown in Fig. 5 and gain insight into the most judicious plan for capturing $\Delta\delta^{13}\text{C}_{\text{max}}$.

In order to test how much of the change in the carbon isotopic signal we observed in evergreen wood is caused by seasonal changes in environmental parameters, we modeled the additive effect of each of these factors as the following:

$$\Delta\delta^{13}\text{C}_{\text{model}} = \Delta\delta^{13}\text{C}_{\text{CO}_2} + A(\Delta P) + B(\Delta T) + C(d) + D(\Delta c_a) + \Delta Y \quad (2)$$

where $\Delta\delta^{13}\text{C}_{\text{model}}$ is the modeled, average seasonal change in $\delta^{13}\text{C}$ resulting from average, seasonal changes in: $\delta^{13}\text{C}_{\text{CO}_2}$ ($\Delta\delta^{13}\text{C}_{\text{CO}_2}$, ‰), precipitation (P , mm), temperature (T , °C), atmospheric CO_2 (c_a , ppm), and post-photosynthetic physiological processes (ΔY , ‰). In order to

Table 3
Climate data.

Location	Maximum $\delta^{13}\text{C}$		Precipitation (mm) ^a		Temperature (°C) ^b		Climate ^c	References
	MJJASO	NDJFMA	P_1	P_2	T_1	T_2		
Mississippi	X		655 ^d	922 ^d	24.8 ^d	13.2 ^d	Temperate	This study
Hawaii	X		146 ^e	256 ^e	14.7 ^e	12.6 ^e	Temperate	This study
Venezuela	X		2109 ^f	1136 ^f	27.0 ^g	26.0 ^g	Tropical	Fichtler et al. (2010)
Italy	X		566	442	13.7	-6.1	Cold	Vaganov et al. (2009)
Sweden	X		411	179	9.7	-5.9	Cold	Vaganov et al. (2009)
Siberia	X		300	193	10.6	-16.2	Cold	Schulze et al. (2004)
Kenya		X	410	680	27.5	24.8	Tropical	Verheyden et al. (2004)
Germany	X		391	389	15.0	-1.4	Cold	Vaganov et al. (2009)
NE Thailand		X	239	864	24.3	29.5	Tropical	Ohashi et al. (2009)
N Thailand		X	142	1047	24.5	27.7	Tropical	Poussart et al. (2004)
SW Australia		X	114	756	22.8	13.8	Temperate	Warren et al. (2001)
Israel	X		19 ^h	185 ^h	28.0	15.0	Arid	Klein et al. (2005)
Elba	X		248	279	28.2	17.5	Temperate	Battipaglia et al. (2010)
Guyana		X	1135	1625	26.3 ⁱ	26.5 ⁱ	Tropical	Pons and Helle (2011)
Pisa	X		391 ^j	506 ^j	19.5 ^j	8.8 ^j	Temperate	De Micco et al. (2007)

Abbreviations: MJJASO = May, June, July, August, September, October; NDJFMA = November, December, January, February, March, April.

^a P_1 and P_2 are defined in Eq. (3) of the text (Section 4).

^b T_1 and T_2 are defined in Eq. (4) of the text (Section 4).

^c Broad climate types are based on Peel et al. (2007).

^d <http://www.weather.com/outlook/health/fitness/wxclimatology/monthly/graph/MSSPNAT:13>.

^e USAFETAC (1990).

^f Instituto Nacional de Meteorología e Hidrología (Station Kilometro 88), http://www.inameh.gob.ve/web/datos_precipitacion/bolivar/Kilometro%2088.pdf.

^g <http://www.weather.com/outlook/health/fitness/wxclimatology/monthly/graph/VEXX0029>.

^h Volcani et al. (2005, Fig. 2, 1999–2001).

ⁱ <http://www.weatherbase.com/weather/weather.php3?s=810010&refer=&units=metric>.

^j <http://www.weather.com/outlook/health/fitness/wxclimatology/monthly/graph/ITXX0059>.

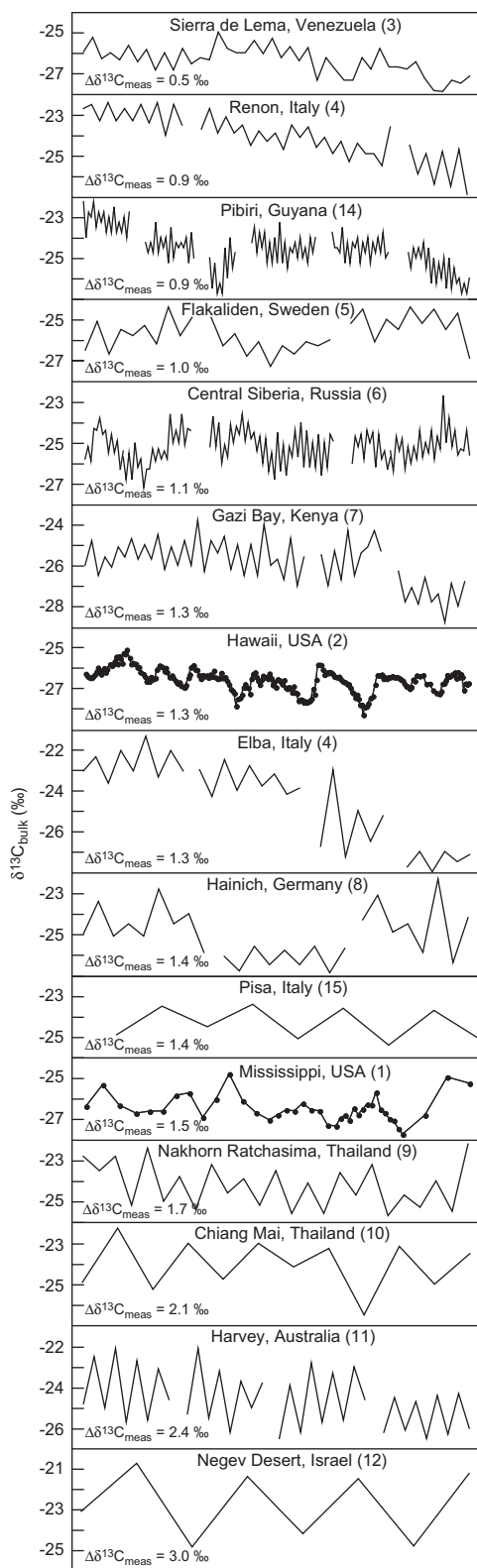


Fig. 4. $\delta^{13}\text{C}_{\text{max}}$ and $\delta^{13}\text{C}_{\text{min}}$ data for each ring plotted for all sites; for samples analyzed as part of this study (Hawaii and Mississippi), individual data points are included. Profiles are arranged in order of increasing $\Delta\delta^{13}\text{C}_{\text{meas}}$ (top to bottom). The site numbers (Table 2) are provided in parentheses next to the site name. Gaps in the profiles indicate where several distinct trees were analyzed.

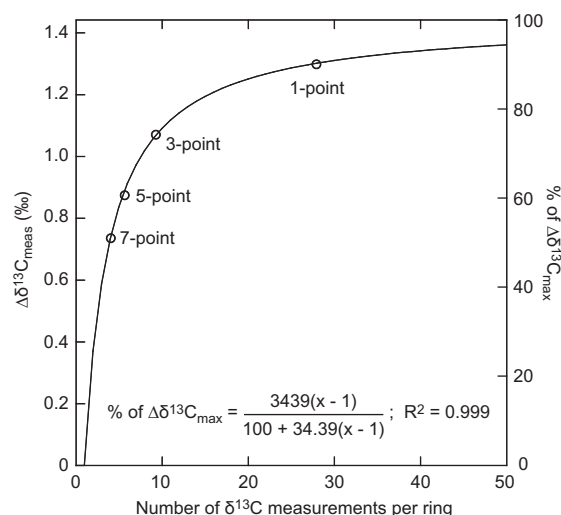


Fig. 5. Relationship between the number of $\delta^{13}\text{C}$ measurements per ring and the average measured change in $\delta^{13}\text{C}$ ($\Delta\delta^{13}\text{C}_{\text{meas}}$) for a *Sophora* tree growing in Hawaii. $\delta^{13}\text{C}$ data were determined at a resolution of 27.9 measurement/ring (1-point). Data for 3-, 5- and 7-point running averages are shown with a hyperbolic curve fit through the data; $\Delta\delta^{13}\text{C}_{\text{meas}} = \Delta\delta^{13}\text{C}_{\text{max}}$ as the number of measurements/ring approaches infinity. For this sample, the hyperbola approaches a value of $\Delta\delta^{13}\text{C}_{\text{meas}} = 1.44\text{‰}$ (i.e., $\Delta\delta^{13}\text{C}_{\text{max}}$). Because $\Delta\delta^{13}\text{C}_{\text{meas}}$ cannot be determined from a single $\delta^{13}\text{C}$ measurement, $\Delta\delta^{13}\text{C}_{\text{meas}} = 0$ at $x = 1$.

capture seasonal differences in light availability, we include the distance from the equator (d , degrees latitude) (Table 4). High latitude sites have a greater change in photosynthetically available radiation (PAR) between summer and winter than low latitude sites (Campbell and Aarup, 1989), therefore seasonal changes in $\delta^{13}\text{C}$ should be partially controlled by latitude. Since increases in PAR cause increases in $\delta^{13}\text{C}$ (Table 1) and maximum PAR occurs in summer, the value for d is defined as being positive when $\delta^{13}\text{C}_{\text{max}}$ occurs in summer and negative when $\delta^{13}\text{C}_{\text{min}}$ occurs in winter. Sites where maximum PAR and $\delta^{13}\text{C}_{\text{max}}$ are out of phase (d is negative) include the Thailand and Guyana sites.

Seasonal changes in the above climate parameters are defined as the following:

$$\Delta P = \ln(P_1) - \ln(P_2) \quad (3)$$

$$\Delta T = T_1 - T_2 \quad (4)$$

where subscripts 1 and 2 indicate the 6-month period (May through October or November through April) during which the maximum and minimum $\delta^{13}\text{C}$ values occurred, respectively (Tables 3 and 4). We used \ln -transformed values of precipitation because values for P_1 and P_2 ranged across more than two orders of magnitude (Table 3). By not transforming the precipitation data, very wet sites would generally appear to have a more seasonal precipitation regime than dry sites (for example, compare Israel to Venezuela). Negative values for ΔP (or ΔT) indicate that precipitation (or temperature) is at its maximum when $\delta^{13}\text{C}$ values are at their minimum. For sites with mean winter temperatures (MWT) below 5°C (Italy, Sweden, Siberia, and Germany), Eq. (4) was solved using both the actual MWT (MWT_{act}) and an adjusted MWT (MWT_{adj}), where $\text{MWT}_{\text{adj}} = 5^\circ\text{C}$,

the temperature below which tree growth ceases (Vaganov et al., 2009). Although tree growth may cease in these cold climates, winter precipitation that falls as snow likely contributes to spring water availability and therefore should affect the $\delta^{13}\text{C}$ value of early wood (Liu et al., 2011). Furthermore, dry season precipitation has been shown to be a primary influence on the $\delta^{13}\text{C}$ value of wood (Koretsune et al., 2009).

Seasonal changes in $\delta^{13}\text{C}_{\text{CO}_2}$ ($\Delta\delta^{13}\text{C}_{\text{CO}_2}$) and c_a (Δc_a) at each site are calculated using data from Keeling et al. (2001) to derive the following equations:

$$\Delta\delta^{13}\text{C}_{\text{CO}_2} = 0.01(x) + 0.13; \quad \text{for } x \geq -8 \quad (5)$$

$$\Delta\delta^{13}\text{C}_{\text{CO}_2} = 0.05; \quad \text{for } x < -8 \quad (6)$$

$$\Delta c_a = 0.23(x) + 4.61; \quad \text{for } x \geq -15 \quad (7)$$

$$\Delta c_a = 1; \quad \text{for } x < -15 \quad (8)$$

where x is latitude (positive values in the northern hemisphere; negative values in southern hemisphere). Eqs. (5) and (7) reflect the empirical observation that $\Delta\delta^{13}\text{C}_{\text{CO}_2}$ and Δc_a increase, from minimum values of 0.05‰ and 1 ppm, with increasing latitude for $x \geq -8$ and $x \geq -15$, respectively (Fig. 6). When $x < -8$ (Eq. (6)), $\Delta\delta^{13}\text{C}_{\text{CO}_2}$ is small ($\sim 0.05\%$) and varies trivially with latitude; therefore $\Delta\delta^{13}\text{C}_{\text{CO}_2}$ was defined as constant and equal to 0.05‰ for these Southern hemisphere sites (Eq. (6)). When $x < -15$ (Eq. (8)), Δc_a is small (~ 1 ppm) and varies trivially with latitude; therefore Δc_a was defined as constant and equal to 1 ppm for these Southern hemisphere sites (Eq. (8)). The signs for $\Delta\delta^{13}\text{C}_{\text{CO}_2}$ and Δc_a are defined as being positive when the maximum $\delta^{13}\text{C}$ and $\delta^{13}\text{C}_{\text{CO}_2}$ (and minimum c_a) values occur in the same season and negative when they occur in opposite seasons (e.g., both Thailand sites, Guyana, and Kenya) (Table 4). On a seasonal cycle, typically c_a is at its minimum when $\delta^{13}\text{C}_{\text{CO}_2}$ is at its maximum; both low c_a and high $\delta^{13}\text{C}_{\text{CO}_2}$ increase $\delta^{13}\text{C}$ (Table 1).

Within Eq. (2), ΔY reflects seasonal changes in post-photosynthetic physiological processes such as remobilization of stored carbon that are independent of climate. A , B , C , and D are scalars where $A \leq 0$, $B \geq 0$, $C \geq 0$, and $D \geq 0$ so that increasing ΔP will decrease $\Delta\delta^{13}\text{C}_{\text{model}}$ (as in Fig. 1b) while increasing ΔT , increasing latitude, and increasing Δc_a will each increase $\Delta\delta^{13}\text{C}_{\text{model}}$. We iteratively optimized Eq. (2) using Excel Solver (Frontline Systems Inc., Nevada, USA) to minimize the sum of the squared differences between $\Delta\delta^{13}\text{C}_{\text{meas}}$ and $\Delta\delta^{13}\text{C}_{\text{model}}$ for all sites using calculated or published $\Delta\delta^{13}\text{C}_{\text{CO}_2}$, ΔP , ΔT , Δc_a , and d data for all 15 sites (Table 4) to obtain the following values for the five constants: $A = -0.82$, $B = 0$, $C = 0$, $D = 0$, and $\Delta Y = 0.73$; optimization using MWT_{act} or MWT_{adj} resulted in identical values for the constants. Although intraring $\delta^{13}\text{C}$ values have been shown to correlate with temperature (Wilson and Grinstead, 1977), the relationship between $\delta^{13}\text{C}$ and temperature can be variable (Schleser et al., 1999); therefore we also optimized Eq. (2) without the constraint of $B \geq 0$. Eliminating this constraint allowed for negative values for B (increased temperatures decrease $\delta^{13}\text{C}$ values), however the effect was small ($< 0.01\%$ per 1°C change in temperature) using both MWT_{act} and MWT_{adj} data. We also converted our temperature data to Kelvin, so that all values were positive; therefore temperature data could be ln-transformed, similar to precipitation. Use of the ln-transformed temperature data did not change any of the values for the constants. Because values ranging from ~ 0.01 to 0.02% /ppm are often cited as the discrimination due to pCO_2 (Feng and Epstein, 1995; Treydte et al., 2001, 2009; McCarroll et al., 2009), we also optimized Eq. (2) setting $D = 0.01$ and $D = 0.02$; however the values for A , B , C , and ΔY (and our R^2 value for the line $\Delta\delta^{13}\text{C}_{\text{meas}} = \Delta\delta^{13}\text{C}_{\text{model}}$) did not change (vs. $D = 0$). Substitution of the constants ($A = -0.82$, $B = 0$, $C = 0$, $D = 0$, $\Delta Y = 0.73$) into Eq. (2) gives:

Table 4
Data for each term input into Eq. (2) used to calculate $\Delta\delta^{13}\text{C}_{\text{model}}$.

Location	d^a ($^\circ$ latitude)	ΔP Eq. (3)	ΔT ($^\circ\text{C}$) Eq. (4)	$\Delta\delta^{13}\text{C}_{\text{CO}_2}^b$ (‰) Eqs. (5) and (6)	Δc_a^c (ppm) Eqs. (7) and (8)	$\Delta\delta^{13}\text{C}_{\text{model}}$ (‰)	$\Delta\delta^{13}\text{C}_{\text{model}} - \Delta\delta^{13}\text{C}_{\text{meas}}$ (‰)
Mississippi	31.60	-0.34	11.6	0.45	11.9	1.47	-0.07
Hawaii	19.83	-0.56	2.1	0.33	9.2	1.53	0.23
Venezuela	6.10	0.62	1.0	0.19	6.0	0.42	-0.10
Italy	46.60	0.25	19.7	0.60	15.4	1.13	0.26
Sweden	64.12	0.83	15.6	0.78	19.5	0.83	-0.13
Siberia	60.72	0.44	26.8	0.75	18.7	1.12	0.03
Kenya	4.42	-0.51	2.6	-0.09	-5.6	1.07	-0.20
Germany	51.07	0.01	16.4	0.65	16.4	1.38	0.01
NE Thailand	-14.50	-1.29	-5.3	-0.28	-1.2	1.52	-0.14
N Thailand	-18.50	-2.00	-3.2	-0.32	-0.3	2.06	0.01
SW Australia	33.97	-1.89	8.1	0.05	1.0	2.35	-0.03
Israel	31.33	-2.30	13.0	0.45	11.9	3.08	0.07
Elba	42.77	-0.12	10.7	0.57	14.5	1.40	0.07
Guyana	-5.03	-0.36	-0.2	-0.18	-3.4	0.85	-0.06
Pisa	43.23	-0.26	10.7	0.57	14.6	1.52	0.09

^a Negative values for d indicate maximum photosynthetically available radiation (PAR) and maximum $\delta^{13}\text{C}$ values occur in opposite seasons.

^b Negative values for $\Delta\delta^{13}\text{C}_{\text{CO}_2}$ indicate maximum $\Delta\delta^{13}\text{C}_{\text{CO}_2}$ and maximum $\delta^{13}\text{C}$ values occur in opposite seasons.

^c Negative values for Δc_a indicate maximum Δc_a and maximum $\delta^{13}\text{C}$ values occur in the same season.

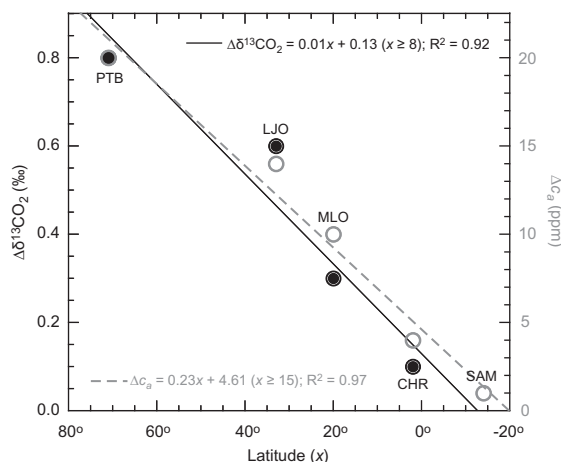


Fig. 6. Relationship showing the strong dependence of seasonal changes in the carbon isotopic composition of CO₂ in the atmosphere ($\Delta\delta^{13}\text{C}_{\text{CO}_2}$, black line) and seasonal changes in the partial pressure of CO₂ in the atmosphere (Δc_a , dashed gray line) on latitude. $\Delta\delta^{13}\text{C}_{\text{CO}_2}$ and Δc_a are calculated as the difference between the maximum and minimum values each year. In the northern hemisphere, high latitude sites show greater Δc_a and $\Delta\delta^{13}\text{C}_{\text{CO}_2}$ than low latitude sites; Δc_a and $\Delta\delta^{13}\text{C}_{\text{CO}_2}$ are minor in the southern hemisphere. PTB – Point Barrow, Alaska, USA; LJO – La Jolla Pier, California, USA; MLO – Mauna Loa Observatory, Hawaii, USA; CHR – Christmas Island; SAM – American Samoa. Data from Keeling et al. (2001).

$$\Delta\delta^{13}\text{C}_{\text{model}} = \Delta\delta^{13}\text{C}_{\text{CO}_2} - 0.82(\Delta P) + 0.73 \quad (9)$$

which results in $R^2 = 0.96$ for the 1:1 line, $\Delta\delta^{13}\text{C}_{\text{meas}} = \Delta\delta^{13}\text{C}_{\text{model}}$ (Fig. 7). Thus the widely different values for $\Delta\delta^{13}\text{C}_{\text{meas}}$ (0.5–3.0‰) in evergreen species growing across the entire latitudinal (DeFries et al., 2000) and climate (Peel et al., 2007) range of evergreen trees (Fig. 2)

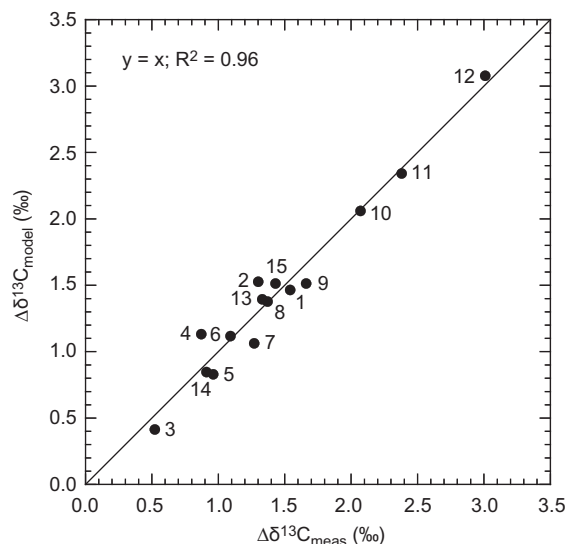


Fig. 7. Correlation between the measured ($\Delta\delta^{13}\text{C}_{\text{meas}}$) and modeled ($\Delta\delta^{13}\text{C}_{\text{model}}$) change in $\delta^{13}\text{C}$ for all 15 sites, demonstrating the potential for $\Delta\delta^{13}\text{C}_{\text{meas}}$ to reconstruct seasonal precipitation. ΔP and $\Delta\delta^{13}\text{C}_{\text{CO}_2}$ are defined in Eqs. (3), (5), and (6). Sites are labeled according to the site numbers listed in Table 2.

can be explained by variations in $\Delta\delta^{13}\text{C}_{\text{CO}_2}$ and ΔP among sites, but is not described by changes in light, temperature, and atmospheric pCO₂ that the tree experiences throughout the year. This optimization implies that $\Delta\delta^{13}\text{C}_{\text{CO}_2}$ and ΔP are the dominant environmental influences on the intra-ring $\delta^{13}\text{C}$ pattern. $\Delta\delta^{13}\text{C}_{\text{meas}}$ did not correlate with $\Delta\delta^{13}\text{C}_{\text{CO}_2}$, ΔT , x , or d ($R^2 \leq 0.10$), but did correlate with ΔP ($R^2 = 0.83$) across all sites (Fig. EA1).

5. DISCUSSION

The optimization of Eq. (2) suggests that temperature, light levels, and atmospheric pCO₂ do not significantly affect the intra-ring $\delta^{13}\text{C}$ pattern of bulk evergreen wood. A lack of a correlation with temperature and light levels (latitude) is consistent with an analysis of $\delta^{13}\text{C}$ values obtained across a global latitudinal gradient (Kelly and Woodward, 1995) and a low-resolution $\delta^{13}\text{C}$ analysis across tree rings (Gebrekirstos et al., 2009). The global collection of sites examined here includes tropical locations that lack large seasonal changes in temperature, incoming solar radiation, $\delta^{13}\text{C}_{\text{CO}_2}$, and c_a (e.g., Venezuela, Kenya, NE Thailand, N Thailand, Guyana, and Hawaii). Yet even among these sites, $\Delta\delta^{13}\text{C}_{\text{meas}}$ ranged greatly (0.5–2.1‰), reinforcing the likelihood that changes in precipitation and resultant water availability is a dominant control over $\Delta\delta^{13}\text{C}_{\text{meas}}$ (Leavitt and Long, 1991; Leavitt, 2002; De Micco et al., 2007). Our results are supported by two recent meta-analyses of $\delta^{13}\text{C}$ values in leaves from hundreds of sites that concluded mean annual precipitation was the strongest predictor of leaf carbon isotope fractionation, with minor effects from temperature and latitude (Diefendorf et al., 2010; Kohn, 2010).

Other researchers have indicated that high-resolution intra-ring $\delta^{13}\text{C}$ values correlate with temperature (Wilson and Grinsted, 1977) or irradiance (Warren et al., 2001; Vaganov et al., 2009). We see a similar connection in our study: in all but three sites (both Thailand sites and Guyana) measured isotopic profiles exhibited the highest $\delta^{13}\text{C}$ values during summer, when temperature and irradiance were at their maximum. This association may be coincidental due to higher $\delta^{13}\text{C}_{\text{CO}_2}$ values in summer for northern hemisphere sites (Keeling et al., 2001), concurrent changes in post-photosynthetic carbon mobilization (the variable, ΔY), or may simply result from correlations between temperature, irradiance, and relative humidity (McCarroll and Loader, 2004). Kitagawa and Wada (1993) hypothesized that changes in $\delta^{13}\text{C}_{\text{CO}_2}$ contributed to changes in $\delta^{13}\text{C}$ through the annual cycle based on the similarity in the shape of measured curves. In contrast, Wilson and Grinsted (1977) and Leavitt and Long (1991) argued against $\delta^{13}\text{C}_{\text{CO}_2}$ control over the intra-annual $\delta^{13}\text{C}$ pattern due to phase and magnitude differences in measured curves. Our analysis allows for $\delta^{13}\text{C}_{\text{CO}_2}$ and $\delta^{13}\text{C}$ to be out of phase (the value for $\Delta\delta^{13}\text{C}_{\text{CO}_2}$ is defined as negative when maximum values for $\delta^{13}\text{C}_{\text{CO}_2}$ and $\delta^{13}\text{C}$ occur in opposite seasons) and suggests that the effect of ΔP accounts for differences between the amplitude of the $\delta^{13}\text{C}_{\text{CO}_2}$ and $\delta^{13}\text{C}$ signals.

In long-term, low-resolution $\delta^{13}\text{C}$ tree-ring records, correlations between climate variables and $\delta^{13}\text{C}$ have been

shown to improve upon correction for increasing $p\text{CO}_2$ (Gagen et al., 2007; Kirilyanov et al., 2008; Loader et al., 2008; Treydte et al., 2009). However, we did not see a significant seasonal fractionation due to seasonal changes in c_a ($D = 0$). This result makes sense given that the carbon isotope fractionation usually used for tree cores is $\sim 0.007\text{‰}/\text{ppm}$ (Treydte et al., 2001) to $0.016\text{‰}/\text{ppm}$ (McCarroll et al., 2009) and Δc_a is less than 20 ppm for all sites (Table 4); therefore, the most that the term $D(\Delta c_a)$ could change $\Delta\delta^{13}\text{C}_{\text{model}}$ would be $\sim 0.1\text{--}0.3\text{‰}$.

Finally, the optimization we described yields $\Delta Y = 0.73\text{‰}$ (Eq. (9)). We suggest that this constant embodies a carbon isotope effect common to the globally distributed sample set of evergreen trees. In particular, the process of starch storage and subsequent remobilization is a process shared by all evergreen trees; Verheyden et al. (2004), Vaganov et al. (2009), and Fichtler et al. (2010) previously proposed that carbon isotope patterns in evergreen wood may be influenced by such cycling of carbon within phytosynthate. Our results support the hypothesis that post-photosynthetic physiological processes, such as remobilization of stored carbon, influence the $\delta^{13}\text{C}$ signal.

6. IMPLICATIONS AND CONCLUSIONS

Twenty years ago, Leavitt and Long (1991) suggested that if seasonal changes in $\delta^{13}\text{C}$ measured across tree rings are ubiquitous and can be explained quantitatively, seasonal reconstructions of past climates could be obtained from fossil wood. We propose that Eq. (9) may be usefully applied as a means to reconstruct the average ratio of summer to winter precipitation from the intra-annual $\delta^{13}\text{C}$ pattern measured within fossil evergreen wood. When taken with independent estimates of mean annual precipitation ($\text{MAP} = P_1 + P_2$), average values for summer and winter precipitation can be quantified. The clear difference in isotopic pattern between deciduous wood and evergreen wood (Fig. 1), including in ancient samples (Jahren and Sternberg, 2008), makes the identification of evergreen wood possible even in cases where no anatomical or other taphonomic information is available. In addition, preservation of distinct tree ring anatomy is not required (Pons and Helle, 2011). Because the dataset used to generate Eq. (9) represents both angiosperm and gymnosperm trees from ten different genera sampled from the full range of latitude and climate under which evergreen trees have been known to exist, we believe it is widely applicable throughout geologic history. $\delta^{13}\text{C}$ values often vary among species (e.g., Kelly and Woodward, 1995; Koretsune et al., 2009) and even individual trees growing under identical conditions (Leavitt, 2002, 2010; Gebrekirstos et al., 2009) (Fig. 4), yet we found no significant difference in $\Delta\delta^{13}\text{C}_{\text{meas}}$ between two distinct genera growing at the Guyana site ($\Delta\delta^{13}\text{C}_{\text{meas}} = 0.88\text{‰}$ and 0.96‰ for *Carapa* and *Goupia*, respectively). Our results suggest that relative changes in $\delta^{13}\text{C}$ measured across tree rings are consistent and predictable for all evergreen species.

Non-permineralized, fossil wood is abundantly available from the Quaternary, including Holocene (Clague et al.,

1992; Ferrio et al., 2006; Noshiro et al., 2007; Tipping et al., 2008; Kaiser et al., 2009) and Pleistocene (Burgh, 1974; Leavitt and Long, 1991; Mijarra et al., 2007) sediments, and has also been documented extensively throughout the Tertiary (Richter et al., 2008) [Pliocene (Martinetto et al., 2007; Vassio et al., 2008; Baldanza et al., 2009), Miocene (Williams et al., 2008; Erdei et al., 2009), Eocene (Jahren, 2007), Paleocene (Blanchette et al., 1991)] and Cretaceous (Gröcke et al., 1999; Yans et al., 2010). This method is particularly applicable to fossil wood pieces because only relative changes in the $\delta^{13}\text{C}$ value are required, thus we may discount any consistent diagenetic alteration or juvenility effects (Gagen et al., 2007, 2008; Esper et al., 2010). Similarly, barring sudden, cataclysmic events that may occur over the span of a few years, estimates of the actual $\delta^{13}\text{C}_{\text{CO}_2}$ value of the ancient atmosphere (McCarroll and Loader, 2004) or changes in c_a over time (McCarroll et al., 2009) are not required. Therefore, although $p\text{CO}_2$ levels have varied greatly throughout the Cenozoic (e.g., Pearson and Palmer, 2000; Demicco et al., 2003; Pagani et al., 2005), ΔP could be calculated for any site in which non-permineralized, evergreen wood is recovered. In addition, such analyses could be conducted on just a limited number of fossil rings; for the modern studies summarized here, at most only four trees were analyzed and nearly half of all studies (7 out of 15) examined twelve or fewer total rings (Table 2). In closing, we recommend that high-resolution $\delta^{13}\text{C}$ measurements across tree rings should become a standard practice for isotopic study of wood, due to the large amount of environmental information that is missed when sampled at lower resolution. If mean annual precipitation could be estimated independently, this method could be used to calculate mean summer and winter precipitation. Consideration of seasonality over mean annual conditions represents an important progression in the field of paleoclimate reconstruction.

ACKNOWLEDGMENTS

We thank W.M. Hagopian, A. Timmermann, and R.J. Panetta for field assistance, laboratory assistance, and other helpful contributions. This work was supported by NSF Grant ARC-08-04573 and DOE/BES Grant DE-FG02-09ER16002.

APPENDIX A. LISTING OF VARIABLES DESCRIBED IN THE ARTICLE

$\delta^{13}\text{C}_{\text{CO}_2}$	carbon isotope ratio of atmospheric CO_2 (‰)
$\delta^{13}\text{C}$	carbon isotope ratio of bulk plant tissue (‰)
$\delta^{13}\text{C}_{\text{max}}$	maximum $\delta^{13}\text{C}$ value measured in a single growth ring (‰)
$\delta^{13}\text{C}_{\text{min}}$	lowest $\delta^{13}\text{C}$ value, prior to $\delta^{13}\text{C}_{\text{max}}$, measured in a single growth ring (‰)
a	fractionation caused by diffusion in air (‰)
b	fractionation caused by enzymatic carboxylation
c_i	intracellular partial pressure of CO_2
c_a	atmospheric partial pressure of CO_2
$\Delta\delta^{13}\text{C}_{\text{meas}}$	average seasonal change in the $\delta^{13}\text{C}$ value measured across 3 or more growth rings (‰); $\Delta\delta^{13}\text{C}_{\text{meas}} = (\delta^{13}\text{C}_{\text{max}} - \delta^{13}\text{C}_{\text{min}})_{\text{avg}}$

$\Delta\delta^{13}\text{C}_{\text{model}}$	seasonal change in $\delta^{13}\text{C}$ modeled across growth rings (‰)
$\Delta\delta^{13}\text{C}_{\text{max}}$	maximum, average seasonal change in $\delta^{13}\text{C}$ that could be measured across a given set of growth rings; $\Delta\delta^{13}\text{C}_{\text{meas}}$ if rings were sub-sectioned at infinite resolution.
$\Delta\delta^{13}\text{C}_{\text{CO}_2}$	seasonal change in $\delta^{13}\text{C}_{\text{CO}_2}$ (‰)
Δc_a	seasonal change in atmosphere partial pressure of CO_2 (ppm)
ΔP	seasonal change in precipitation (dimensionless)
P_1	6-month (May through October or November through April) total precipitation during which $\delta^{13}\text{C}_{\text{max}}$ occurs (mm)
P_2	6-month (May through October or November through April) total precipitation during which $\delta^{13}\text{C}_{\text{min}}$ occurs (mm)
ΔT	seasonal change in temperature ($^{\circ}\text{C}$)
T_1	6-month (May through October or November through April) average temperature during which $\delta^{13}\text{C}_{\text{max}}$ occurs ($^{\circ}\text{C}$)
T_2	6-month (May through October or November through April) average temperature during which $\delta^{13}\text{C}_{\text{min}}$ occurs ($^{\circ}\text{C}$)
MWT_{act}	actual mean winter temperature ($^{\circ}\text{C}$)
MWT_{adj}	adjusted mean winter temperature (5°C)
A	constant scalar for seasonal change in precipitation ($A \leq 0\text{‰}$)
B	constant scalar for seasonal change in temperature ($B \geq 0\text{‰}/^{\circ}\text{C}$)
C	constant scalar for seasonal change in latitude ($C \geq 0\text{‰}/\text{degree latitude}$)
D	constant scalar for seasonal change in atmospheric partial pressure of CO_2 ($D \geq 0$ or $0.02 \geq D \geq 0.01$, $\text{‰}/\text{ppm}$)
ΔY	seasonal changes in $\delta^{13}\text{C}$ caused by post-photosynthetic physiological processes (‰)
d	distance from the equator (degrees latitude; positive when $\delta^{13}\text{C}_{\text{max}}$ occurs in summer, negative when $\delta^{13}\text{C}_{\text{max}}$ occurs in winter)
x	latitude (degrees; Northern hemisphere, positive values; Southern hemisphere, negative values)

APPENDIX B. SUPPLEMENTARY DATA

Supplementary data associated with this article can be found, in the online version, at doi:10.1016/j.gca.2011.08.002.

REFERENCES

- Aranda I., Pardos M., Puértolas J., Jiménez M. D. and Pardos J. A. (2007) Water-use efficiency in cork oak (*Quercus suber*) is modified by the interaction of water and light availabilities. *Tree Physiol.* **27**, 671–677.
- Arens N. C., Jahren A. H. and Amundson R. (2000) Can C3 plants faithfully record the carbon isotopic composition of atmospheric carbon dioxide? *Paleobiology* **26**, 137–164.
- Baldanza A., Sabatino G., Triscari M. and De Angelis M. C. (2009) The Dunarobba Fossil Forest (Umbria, Italy): mineralogical transformations evidences as possible decay effects. *Period. Mineral.* **78**, 51–60.
- Barbour M. M., Walcroft A. S. and Farquhar G. D. (2002) Seasonal variation in $\delta^{13}\text{C}$ and $\delta^{18}\text{O}$ of cellulose from growth rings of *Pinus radiata*. *Plant Cell Environ.* **25**, 1483–1499.
- Battipaglia G., De Micco V., Brand W. A., Linke P., Aronne G., Saurer M. and Cherubini P. (2010) Variations of vessel diameter and $\delta^{13}\text{C}$ in false rings of *Arbutus unedo* L. reflect different environmental conditions. *New Phytol.* **188**, 1099–1112.
- Blanchette R. A., Cease K. R., Abad A. R., Burnes T. A. and Obst J. R. (1991) Ultrastructural characterization of wood from Tertiary fossil forests in the Canadian Arctic. *Can. J. Bot.* **69**, 560–568.
- Bowling D. R., McDowell N. G., Bond B. J., Law B. E. and Ehleringer J. R. (2002) ^{13}C content of ecosystem respiration is linked to precipitation and vapor pressure deficit. *Oecologia* **131**, 113–124.
- Brodribb T. J. and McAdam S. A. M. (2011) Passive origins of stomatal control in vascular plants. *Science* **331**, 582–585.
- Buckley B. M., Anchukaitis K. J., Penny D., Fletcher R., Cook E. R., Sano M., Nam L. C., Wichienkeo A., Minh T. T. and Hong T. M. (2010) Climate as a contributing factor in the demise of Angkor, Cambodia. *Proc. Natl. Acad. Sci. USA* **107**, 6748–6752.
- Burgh J. v. D. (1974) Wood-remains from the Lower Pleistocene of Tegelen (The Netherlands). *Scripta Geol.* **25**, 1–35.
- Campbell J. W. and Aarup T. (1989) Photosynthetically available radiation at high latitudes. *Limnol. Oceanogr.* **34**, 1490–1499.
- Cernusak L. A., Winter K. and Turner B. L. (2009) Physiological and isotopic ($\delta^{13}\text{C}$ and $\delta^{18}\text{O}$) responses of three tropical tree species to water and nutrient availability. *Plant Cell Environ.* **32**, 1441–1455.
- Cherubini P., Fontana G., Rigling D., Dobbertin M., Brang P. and Innes J. L. (2002) Tree-life history prior to death: two fungal root pathogens affect tree-ring growth differently. *J. Ecol.* **90**, 839–850.
- Cherubini P., Gartner B. L., Tognetti R., Braker O. U., Schoch W. and Innes J. L. (2003) Identification, measurement and interpretation of tree rings in woody species from mediterranean climates. *Biol. Rev.* **78**, 119–148.
- Clague J. J., Mathewes R. W., Buhay W. M. and Edwards T. W. D. (1992) Early Holocene climate at Castle Peak, South Coast Mountains, British Columbia, Canada. *Palaeogeogr. Palaeoclimatol. Palaeoecol.* **95**, 153–167.
- Currey D. R. (1965) An ancient bristlecone pine stand in Eastern Nevada. *Ecology* **46**, 564–566.
- Dawson T. E., Mambelli S., Plamboeck A. H., Templer P. H. and Tu K. P. (2002) Stable isotopes in plant ecology. *Annu. Rev. Ecol. Syst.* **33**, 507–559.
- De Micco V., Saurer M., Aronne G., Tognetti R. and Cherubini P. (2007) Variations of wood anatomy and $\delta^{13}\text{C}$ within-tree rings of coastal *Pinus pinaster* showing intra-annual density fluctuations. *IWA J.* **28**, 61–74.
- Defries R. S., Hansen M. C., Townshend J. R. G., Janetos A. C. and Loveland T. R. (2000) A new global 1-km dataset of percentage tree cover derived from remote sensing. *Global Change Biol.* **6**, 247–254.
- Demico R. V., Lowenstein T. K. and Hardie L. A. (2003) Atmospheric pCO_2 since 60 Ma from records of seawater pH, calcium, and primary carbonate mineralogy. *Geology* **31**, 793–796.
- Diefendorf A. F., Mueller K. E., Wing S. L., Koch P. L. and Freeman K. H. (2010) Global patterns in leaf ^{13}C discrimination and implications for studies of past and future climate. *Proc. Natl. Acad. Sci.* **107**, 5738–5743.

- Edwards T. W. D., Graf W., Trumborn P., Stichler W., Lipp J. and Payer H. D. (2000) $\delta^{13}\text{C}$ response surface resolves humidity and temperature signals in trees. *Geochim. Cosmochim. Acta* **64**, 161–167.
- Ehleringer J. R. and Cooper T. A. (1988) Correlations between carbon isotope ratio and microhabitat in desert plants. *Oecologia* **76**, 562–566.
- Ehleringer J. R., Field C. B., Lin Z.-F. and Kuo C.-Y. (1986) Leaf carbon isotope and mineral composition in subtropical plants along an irradiance cline. *Oecologia* **70**, 520–526.
- Eilmann B., Buchmann N., Siegwolf R., Saurer M., Cherubini P. and Rigling A. (2010) Fast response of Scots pine to improved water availability reflected in tree-ring width and $\delta^{13}\text{C}$. *Plant Cell Environ.* **33**, 1351–1360.
- Erdei B., Dolezych M. and Hably L. (2009) The buried Miocene forest at Bükkábrány, Hungary. *Rev. Palaeobot. Palynol.* **155**, 69–79.
- Esper J., Frank D. C., Battipaglia G., Büntgen U., Holert C., Treydte K., Siegwolf R. and Saurer M. (2010) Low-frequency noise in $\delta^{13}\text{C}$ and $\delta^{18}\text{O}$ tree ring data: a case study of *Pinus uncinata* in the Spanish Pyrenees. *Global Biogeochem. Cycles* **24**, GB4018.
- Farquhar G. D., Ehleringer J. R. and Hubick K. T. (1989) Carbon isotope discrimination and photosynthesis. *Annu. Rev. Plant Physiol. Plant Mol. Biol.* **40**, 503–537.
- Farquhar G. D., O'leary M. H. and Berry J. A. (1982) On the relationship between carbon isotope discrimination and intercellular carbon dioxide concentration in leaves. *Aust. J. Plant Physiol.* **9**, 121–137.
- Feng X. and Epstein S. (1995) Carbon isotopes of trees from arid environments and implications for reconstructing atmospheric CO_2 concentration. *Geochim. Cosmochim. Acta* **59**, 2599–2608.
- Ferrio J. P., Alonso N., Lopez J. B., Araus J. L. and Voltas J. (2006) Carbon isotope composition of fossil charcoal reveals aridity changes in the NW Mediterranean Basin. *Global Change Biol.* **12**, 1253–1266.
- Fichtler E., Helle G. and Worbes M. (2010) Stable-carbon isotope time series from tropical tree rings indicate a precipitation signal. *Tree-Ring Res.* **66**, 35–49.
- Gagen M., McCarroll D., Loader N. J., Robertson L., Jalkanen R. and Anchukaitis K. J. (2007) Exorcising the 'segment length curse': summer temperature reconstruction since AD 1640 using non-detrended stable carbon isotope ratios from pine trees in northern Finland. *Holocene* **17**, 435–446.
- Gagen M., McCarroll D., Robertson I., Loader N. J. and Jalkanen R. (2008) Do tree ring $\delta^{13}\text{C}$ series from *Pinus sylvestris* in northern Fennoscandia contain long-term non-climatic trends? *Chem. Geol.* **252**, 42–51.
- Galle A., Esper J., Feller U., Ribas-Carbo M. and Fonti P. (2010) Responses of wood anatomy and carbon isotope composition of *Quercus pubescens* saplings subjected to two consecutive years of summer drought. *Ann. For. Sci.* **67**.
- Gebrekirstos A., Van Noordwijk M., Neufeldt H. and Mitlöhner R. (2011) Relationships of stable carbon isotopes, plant water potential and growth: an approach to assess water use efficiency and growth strategies of dry land agroforestry species. *Trees-Struct. Funct.* **25**, 95–102.
- Gebrekirstos A., Worbes M., Teketay D., Fetene M. and Mitlöhner R. (2009) Stable carbon isotope ratios in tree rings of co-occurring species from semi-arid tropics in Africa: patterns and climatic signals. *Global Planet. Change* **66**, 253–260.
- Gröcke D. R., Hesselbo S. P. and Jenkyns H. C. (1999) Carbon isotope composition of Lower Cretaceous fossil wood: ocean-atmosphere chemistry and relation to sea-level change. *Geology* **27**, 155–158.
- Grudd H., Briffa K. R., Karlén W., Bartholin T. S., Jones P. D. and Kromer B. (2002) A 7400-year tree-ring chronology in northern Swedish Lapland: natural climatic variability expressed on annual to millennial timescales. *Holocene* **12**, 657.
- Helle G. and Schleser G. H. (2004) Beyond CO_2 -fixation by Rubisco – an interpretation of $^{13}\text{C}/^{12}\text{C}$ variations in tree rings from novel intra-seasonal studies on broad-leaf trees. *Plant Cell Environ.* **27**, 367–380.
- Hughes M. K., Schweingruber F. H., Cartwright D. and Kelly P. M. (1984) July–August temperature at Edinburgh between 1721 and 1975 from tree-ring density and width data. *Nature* **308**, 341–344.
- Jahren A. H. (2007) The Arctic forest of the middle Eocene. *Ann. Rev. Earth Planet. Sci.* **35**, 509–540.
- Jahren A. H. and Sternberg L. S. L. (2008) Annual patterns within tree rings of the Arctic middle Eocene (ca. 45 Ma): isotopic signatures of precipitation, relative humidity, and deciduousness. *Geology* **36**, 99–102.
- Jędrysek M. O., Krąpiec M., Skrzypek G. and Kałużny A. (2003) Air-pollution effect and paleotemperature scale versus $\delta^{13}\text{C}$ records in tree rings and in a peat core (Southern Poland). *Water Air Soil Pollut.* **145**, 359–375.
- Kagawa A. (2003) Effects of spatial and temporal variability in soil moisture on widths and $\delta^{13}\text{C}$ values of eastern Siberian tree rings. *J. Geophys. Res.* **108**.
- Kaiser K., Opgenoorth L., Schoch W. H. and Miehe G. (2009) Charcoal and fossil wood from palaeosols, sediments and artificial structures indicating Late Holocene woodland decline in southern Tibet (China). *Quatern. Sci. Rev.* **28**, 1539–1554.
- Keeling C. D., Piper S. C., Bacastow R. B., Wahlen M., Whorf T. P., Heimann M. and Meijer H. A. (2001) *Exchanges of Atmospheric CO_2 and $^{13}\text{CO}_2$ with the Terrestrial Biosphere and Oceans from 1978 to 2000. I. Global Aspects*. Scripps Institution of Oceanography, San Diego.
- Kelly C. K. and Woodward F. I. (1995) Ecological correlates of carbon isotope composition of leaves: a comparative analysis testing for the effects of temperature, CO_2 and O_2 partial pressures and taxonomic relatedness on $\delta^{13}\text{C}$. *J. Ecol.* **83**, 509–515.
- Kirdyanov A. V., Treydte K. S., Nikolaev A., Helle G. and Schleser G. H. (2008) Climate signals in tree-ring width, density and $\delta^{13}\text{C}$ from larches in Eastern Siberia (Russia). *Chem. Geol.* **252**, 31–41.
- Kitagawa H. and Wada H. (1993) Seasonal and secular $\delta^{13}\text{C}$ variations in annual growth rings of a Japanese cedar tree from Mt. Amagi, Izu Peninsula, Central Japan. *Geochem. J.* **27**, 391–396.
- Klein T., Hemming D., Lin T. B., Grünzweig J. M., Maseyk K., Rotenberg E. and Yakir D. (2005) Association between tree-ring and needle $\delta^{13}\text{C}$ and leaf gas exchange in *Pinus halepensis* under semi-arid conditions. *Oecologia* **144**, 45–54.
- Kohn M. J. (2010) Carbon isotope compositions of terrestrial C3 plants as indicators of (paleo)ecology and (paleo)climate. *Proc. Natl. Acad. Sci. USA* **107**, 19691–19695.
- Koretsune S., Fukuda K., Chang Z., Shi F. and Ishida A. (2009) Effective rainfall seasons for interannual variation in $\delta^{13}\text{C}$ and tree-ring width in early and late wood of Chinese pine and black locust on the Loess Plateau, China. *J. For. Res.* **14**, 88–94.
- Körner C., Farquhar G. D. and Wong S. C. (1991) Carbon isotope discrimination by plants follows latitudinal and altitudinal trends. *Oecologia* **88**, 30–40.
- Kraft R. A., Jahren A. H. and Saudek C. D. (2008) Clinical-scale investigation of stable isotopes in human blood: $\delta^{13}\text{C}$ and $\delta^{15}\text{N}$ from 406 patients at the Johns Hopkins Medical Institutions. *Rapid Commun. Mass Spectrom.* **22**, 3683–3692.

- Kranabetter J. M., Simard S. W., Guy R. D. and Coates K. D. (2010) Species patterns in foliar nitrogen concentration, nitrogen content and ^{13}C abundance for understory saplings across light gradients. *Plant Soil* **327**, 389–401.
- Lara A. and Villalba R. (1993) A 3620-year temperature record from *Fitzroya cupressoides* tree rings in southern South America. *Science* **260**, 1104–1106.
- Leavitt S. W. (2002) Prospects for reconstruction of seasonal environment from tree-ring $\delta^{13}\text{C}$: baseline findings from the Great Lakes area, USA. *Chem. Geol.* **192**, 47–58.
- Leavitt S. W. (2007) Regional expression of the 1988 U.S. Midwest drought in seasonal $\delta^{13}\text{C}$ of tree rings. *J. Geophys. Res.* **112**, D06107.
- Leavitt S. W. (2010) Tree-ring C–H–O isotope variability and sampling. *Sci. Total Environ.* **48**, 5244–5253.
- Leavitt S. W. and Long A. (1991) Seasonal stable-carbon isotope variability in tree rings: possible paleoenvironmental signals. *Chem. Geol. (Isotope Geosci. Sec.)* **87**, 59–70.
- Liu X., Zhao L., Chen T., Shao X., Liu Q., Hou S., Qin D. and An W. (2011) Combined tree-ring width and $\delta^{13}\text{C}$ to reconstruct snowpack depth: a pilot study in the Gongga Mountain, west China. *Theor. Appl. Climatol.* **103**, 133–144.
- Loader N. J., Santillo P. M., Woodman-Ralph J. P., Rolfe J. E., Hall M. A., Gagen M., Robertson I., Wilson R., Froyd C. A. and McCarroll D. (2008) Multiple stable isotopes from oak trees in southwestern Scotland and the potential for stable isotope dendroclimatology in maritime climatic regions. *Chem. Geol.* **252**, 62–71.
- Martinetto E., Scardia G. and Varrone D. (2007) Magnetobios-tratigraphy of the Stura di Lanzo fossil forest succession (Piedmont, Italy). *Riv. Ital. Paleontol. Stratigr.* **113**, 109–125.
- McCarroll D., Gagen M., Loader N. J., Robertson I., Anchukaitis K. J., Los S., Young G. H. F., Jalkanen R., Kirchhefer A. and Waterhouse J. S. (2009) Correction of tree ring stable isotope chronologies for changes in the carbon dioxide content of the atmosphere. *Geochim. Cosmochim. Acta* **73**, 1539–1547.
- McCarroll D., Jalkanen R., Hicks S., Tuovinen M., Gagen M., Pawellek F., Eckstein D., Schmitt U., Autio J. and Heikkinen O. (2003) Multiproxy dendroclimatology: a pilot study in northern Finland. *Holocene* **13**, 829.
- McCarroll D. and Loader N. J. (2004) Stable isotopes in tree rings. *Quatern. Sci. Rev.* **23**, 771–801.
- McCarroll D. and Pawellek F. (2001) Stable carbon isotope ratios of *Pinus sylvestris* from northern Finland and the potential for extracting a climate signal from long Fennoscandian chronologies. *Holocene* **11**, 517–526.
- Mijarra J. M. P., Burjachs F., Manzanque F. G. and Morla C. (2007) A palaeoecological interpretation of the lower-middle Pleistocene Cal Guardiola site (Terrassa, Barcelona, NE Spain) from the comparative study of wood and pollen samples. *Rev. Palaeobot. Palynol.* **146**, 247–264.
- Nakatsuka T., Ohnishi K., Hara T., Sumida A., Mitsuishi D., Kurita N. and Uemura S. (2004) Oxygen and carbon isotopic ratios of tree-ring cellulose in a conifer-hardwood mixed forest in northern Japan. *Chem. J.* **38**, 77–88.
- Norström E., Holmgren K. and Mörth C. M. (2005) Rainfall-driven variations in $\delta^{13}\text{C}$ composition and wood anatomy of *Breonadia salicina* trees from South Africa between AD 1375 and 1995. *S. Afr. J. Sci.* **101**, 162–168.
- Noshiro S., Suzuki M. and Sasaki Y. (2007) Importance of *Rhus verniciflua* Stokes (lacquer tree) in prehistoric periods in Japan, deduced from identification of its fossil woods. *Veg. Hist. Archaeobot.* **16**, 405–411.
- Oberhuber W., Thomaser G., Mayr S. and Bauer H. (1999) Radial growth of Norway spruce infected by *Chrysomyxa rhododendri*. *Phyton-Ann. Rei Bot.* **39**, 147–154.
- Ohashi S., Okada N., Nobuchi T., Siripatanadilok S. and Veenin T. (2009) Detecting invisible growth rings of trees in seasonally dry forests in Thailand: isotopic and wood anatomical approaches. *Trees-Struct. Funct.* **23**, 813–822.
- Pagani M., Zachos J. C., Freeman K. H., Tiplle B. and Bohaty S. (2005) Marked decline in atmospheric carbon dioxide concentrations during the Paleogene. *Science* **309**, 600–603.
- Pearson P. N. and Palmer M. R. (2000) Atmospheric carbon dioxide concentrations over the past 60 million years. *Nature* **406**, 695–699.
- Peel M. C., Finlayson B. L. and McMahon T. A. (2007) Updated world map of the Köppen-Geiger climate classification. *Hydrol. Earth Sys. Sci.* **11**, 1633–1644.
- Piutti E. and Cescatti A. (1997) A quantitative analysis of the interactions between climatic response and intraspecific competition in European beech. *Can. J. For. Res.* **27**, 277–284.
- Pons T. L. and Helle G. (2011) Identification of anatomically non-distinct annual rings in tropical trees using stable isotopes. *Trees-Struct. Funct.* **25**, 83–93.
- Poussart P. F., Evans M. N. and Schrag D. P. (2004) Resolving seasonality in tropical trees: multi-decade, high-resolution oxygen and carbon isotope records from Indonesia and Thailand. *Earth Planet. Sci. Lett.* **218**, 301–316.
- Prapaipong P., Enssle C. W., Morris J. D., Shock E. L. and Lindvall R. E. (2008) Rapid transport of anthropogenic lead through soils in southeast Missouri. *Appl. Geochem.* **23**, 2156–2170.
- Richter S. L., Johnson A. H., Dranoff M. M., Lepage B. A. and Williams C. J. (2008) Oxygen isotope ratios in fossil wood cellulose: isotopic composition of Eocene to Holocene-aged cellulose. *Geochim. Cosmochim. Acta* **72**, 2744–2753.
- Roden J. S., Johnstone J. A. and Dawson T. E. (2009) Intra-annual variation in the stable oxygen and carbon isotope ratios of cellulose in tree rings of coast redwood (*Sequoia sempervirens*). *Holocene* **19**, 189–197.
- Schleser G. H., Helle G., Lücke A. and Vos H. (1999) Isotope signals as climate proxies: the role of transfer functions in the study of terrestrial archives. *Quatern. Sci. Rev.* **18**, 927–943.
- Schulze B., Wirth C., Linke P., Brand W. A., Kuhlmann I., Horna V. and Schulze E. D. (2004) Laser ablation-combustion-GC-IRMS – a new method for online analysis of intra-annual variation of $\delta^{13}\text{C}$ in tree rings. *Tree Physiol.* **24**, 1193–1201.
- Sheu D. D., Kou P., Chiu C.-H. and Chen M.-J. (1996) Variability of tree-ring $\delta^{13}\text{C}$ in Taiwan fir: growth effect and response to May–October temperatures. *Geochim. Cosmochim. Acta* **60**, 171–177.
- Solanki S. K., Usoskin I. G., Kromer B., Schussler M. and Beer J. (2004) Unusual activity of the Sun during recent decades compared to the previous 11,000 years. *Nature* **431**, 1084–1087.
- Stahle D. W. (1999) Useful strategies for the development of tropical tree-ring chronologies. *IAWA J.* **20**, 249–253.
- Stahle D. W., Villanueva Diaz J., Burnette D. J., Paredes J. C., Heim, Jr., R. R., Fye F. K., Soto R. A., Therrell M. D., Cleaveland M. K. and Stahle D. K. (2011) Major Mesoamerican droughts of the past millenium. *Geophys. Res. Lett.* **38**, L05703.
- Suess H. E. (1980) The radiocarbon record in tree rings of the last 8000 years. *Radiocarbon* **22**, 200–209.
- Till C. and Guiot J. (1990) Reconstruction of precipitation in Morocco since 1100 A.D. based on *Cedrus atlantica* tree-ring widths. *Quatern. Res.* **33**, 337–351.
- Tipping R., Ashmore P., Davies A. L., Haggart B. A., Moir A., Newton A., Sands R., Skinner T. and Tisdall E. (2008) Prehistoric *Pinus* woodland dynamics in an upland landscape in northern Scotland: the roles of climate change and human impact. *Veg. Hist. Archaeobot.* **17**, 251–267.

- Toft N. L., Anderson J. E. and Nowak R. S. (1989) Water use efficiency and carbon isotope composition of plants in a cold desert environment. *Oecologia* **80**, 11–18.
- Tognetti R., Cherubini P. and Innes J. L. (2000) Comparative stem-growth rates of Mediterranean trees under background and naturally enhanced ambient CO_2 concentrations. *New Phytol.* **146**, 59–74.
- Tommasini S., Davies G. R. and Elliott T. (2000) Lead isotope composition of tree rings as bio-geochemical tracers of heavy metal pollution: a reconnaissance study from Firenze, Italy. *Appl. Geochem.* **15**, 891–900.
- Treydte K., Schleser G. H., Schweingruber F. H. and Winiger M. (2001) The climatic significance of $\delta^{13}\text{C}$ in subalpine spruces (Lötschental, Swiss Alps): a case study with respect to altitude, exposure and soil moisture. *Tellus B* **53**, 593–611.
- Treydte K. S., Frank D. C., Saurer M., Helle G., Schleser G. H. and Esper J. (2009) Impact of climate and CO_2 on a millennium-long tree-ring carbon isotope record. *Geochim. Cosmochim. Acta* **73**, 4635–4647.
- USAFETAC (1990) Surface observation climatic summaries (SOCS) for Bradshaw AAF Hawaii. United States Air Force Environmental Technical Applications Center, USAFETAC/DS-90/225.
- Vaganov E. A., Schulze E. D., Skomarkova M. V., Knohl A., Brand W. A. and Roscher C. (2009) Intra-annual variability of anatomical structure and $\delta^{13}\text{C}$ values within tree rings of spruce and pine in alpine, temperate and boreal Europe. *Oecologia* **161**, 729–745.
- Van de Water P. K., Leavitt S. W. and Betancourt J. L. (1994) Trends in stomatal density and $^{13}\text{C}/^{12}\text{C}$ ratios of *Pinus flexilis* needles during last glacial–interglacial cycle. *Science* **264**, 239–243.
- Vassio E., Martinetto E., Dolezych M. and Van der Burgh J. (2008) Wood anatomy of the *Glyptostrobus europaeus* “whole-plant” from a Pliocene fossil forest of Italy. *Rev. Palaeobot. Palynol.* **151**, 81–89.
- Verheyden A., Helle G., Schleser G. H., Dehairs F., Beeckman H. and Koedam N. (2004) Annual cyclicity in high-resolution stable carbon and oxygen isotope ratios in the wood of the mangrove tree *Rhizophora mucronata*. *Plant Cell Environ.* **27**, 1525–1536.
- Verheyden A., Roggeman M., Bouillon S., Elskens M., Beeckman H. and Koedam N. (2005) Comparison between $\delta^{13}\text{C}$ of α -cellulose and bulk wood in the mangrove tree *Rhizophora mucronata*: implications for dendrochemistry. *Chem. Geol.* **219**, 275–282.
- Volcani A., Karnieli A. and Svoray T. (2005) The use of remote sensing and GIS for spatio-temporal analysis of the physiological state of a semi-arid forest with respect to drought years. *For. Ecol. Manage.* **215**, 239–250.
- Walcroft A. S., Silvester W. B., Whitehead D. and Kelliher F. M. (1997) Seasonal changes in stable carbon isotope ratios within annual rings of *Pinus radiata* reflect environmental regulation of growth processes. *Aust. J. Plant Physiol.* **24**, 57–68.
- Walia A., Guy R. D. and White B. (2010) Carbon isotope discrimination in western hemlock and its relationship to mineral nutrition and growth. *Tree Physiol.* **30**, 728–740.
- Warren C. R., McGrath J. F. and Adams M. A. (2001) Water availability and carbon isotope discrimination in conifers. *Oecologia* **127**, 476–486.
- Williams C. J., Mendell E. K., Murphy J., Court W. M., Johnson A. H. and Richter S. L. (2008) Paleoenvironmental reconstruction of a Middle Miocene forest from the western Canadian Arctic. *Palaeogeogr. Palaeoclimatol. Palaeoecol.* **261**, 160–176.
- Wilson A. T. and Grinsted M. J. (1977) $^{12}\text{C}/^{13}\text{C}$ in cellulose and lignin as palaeothermometers. *Nature* **265**, 133–135.
- Yans J., Gerards T., Gerienne P., Spagna P., Dejax J., Schnyder J., Storme J.-Y. and Keppens E. (2010) Carbon-isotope analysis of fossil wood and dispersed organic matter from the terrestrial Wealden facies of Hautrage (Mons Basin, Belgium). *Palaeogeogr. Palaeoclimatol. Palaeoecol.* **291**, 85–105.
- Yin C. Y., Pang X. Y. and Chen K. (2009) The effects of water, nutrient availability and their interaction on the growth, morphology and physiology of two poplar species. *Environ. Exp. Bot.* **67**, 196–203.
- Yin C. Y., Wang X., Duan B. L., Luo J. X. and Li C. Y. (2005) Early growth, dry matter allocation and water use efficiency of two sympatric *Populus* species as affected by water stress. *Environ. Exp. Bot.* **53**, 315–322.
- Young G. H. F., McCarroll D., Loader N. J. and Kirchhefer A. J. (2010) A 500-year record of summer near-ground solar radiation from tree-ring stable carbon isotopes. *Holocene* **20**, 315–324.
- Zimmerman J. K. and Ehleringer J. R. (1990) Carbon isotope ratios are correlated with irradiance levels in the Panamanian orchid *Catasetum viridiflavum*. *Oecologia* **83**, 247–249.

Associate editor: Juske Horita